INTERNATIONAL ATOMIC ENERGY AGENCY
UNITED NATIONS EDUCATIONAL, SCIENTIFIC AND CULTURAL ORGANIZATION

INTERNATIONAL CENTRE FOR THEORETICAL PHYSICS
34100 TRIESTE (ITALY) - P.O.B. 586 - MIRAMARE - STRADA COSTIERA 11 - TELEPHONE: 2240-1
CABLE: CENTRATOM - TELEX 460892-I

H4.SMR/204 - 36

WINTER COLLEGE ON

ATOMIC AND MOLECULAR PHYSICS

(9 March - 3 April 1987)

MEDICAL DIAGNOSTICS

S. SVANBERG

Lund Institute of Technology
S-221 00 Lund
Sweden

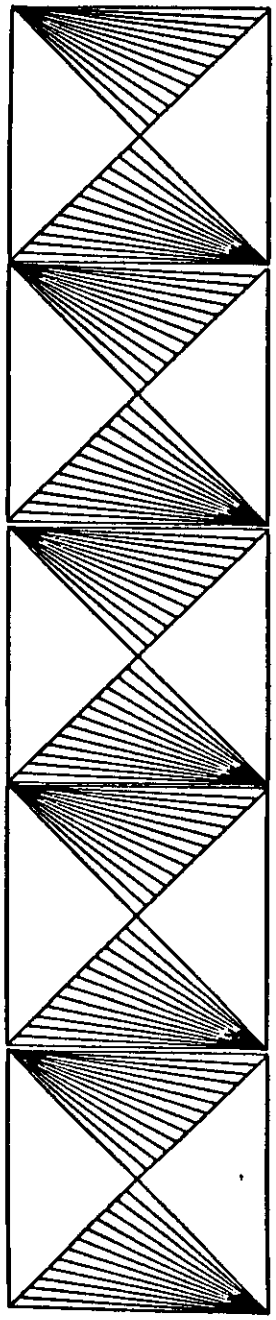

ICALEO '84

Proceedings

Sponsored By
LASER INSTITUTE OF AMERICA

NOVEMBER 12-15, 1984
Boston Marriott/
Copley Place
An Applications Conference With In Depth
Symposia and Professional Advancement Courses

VOLUME 43 — MEDICINE & BIOLOGY

Spectral Characteristics in Tissue Diagnostics using Laser-Induced Fluorescence

J. Ankerst*, S. Montán*, E. Sjöholm*, K. Svanberg* and S. Svanberg*

* Department of Physics, Lund Institute of Technology, P.O. Box 118, S-221 00 LUND, Sweden

* Wallenberg Laboratory and Department of Internal Medicine, Lund University Hospital, S-221 85 LUND, Sweden

Abstract

Extensive studies of laser-induced fluorescence in rat tissues, including cancer tumours have been performed. Contrast enhancement techniques have been developed which greatly improve the ability to localize a tumour when using fluorescence from the tumour-seeking substance hematoporphyrin derivative (HPD). A multi-colour fluorescence imaging technique has been tested. A discussion of clinical applications is also included in this paper.

Introduction

Using UV light, fluorescence with a certain intensity and spectral distribution can be induced in almost any material. This fluorescence can sometimes be used for characterizing the sample. We are presently involved in a research program on the utilization of laser-induced fluorescence (LIF) for gaining information on tissue. In particular, we are investigating the possibility of detecting malignancies in unprepared tissue as well as in tissue which has been subject to previous systemic injection of hematoporphyrin derivative (HPD). It is well established that HPD is selectively retained by tumour tissue[1]. The characteristic HPD fluorescence in the red spectral region can be used for tumour detection e.g. in endoscopic investigations of the lung[2,3] and bladder[4,5]. The HPD-assisted photochemical destruction of tumours following irradiation with red light (630 nm) is a further attractive possibility[1,6].

In tumour localization the natural tissue fluorescence can be strong and varying in spectral distribution and it is thus very important to fully utilize the spectral signature of malignant tissue in a contrast enchancement procedure. When HPD is used for tumour localization it is desirable to be able to detect tumours even with low doses of HPD because of the photosensibilization to ambient light. With optimized spectral information processing it might be possible to substantially cut down the normally required 4 weeks of reduced light exposure. We have studied the spectral characteristics of HPD-bearing tissue of various kinds in extensive experiments on rats with induced tumours.

It would be very convenient to be able to use the natural tissue fluorescence itself for tumour localization, and preliminary experiments on various tissues in rats, pigs and humans have been performed. In particular, human brain-, bladder- and skin tumours have been investigated.

In our experiments we have mostly used pulsed N_2 lasers in conjunction with diode- array detector techniques. Point measurements with full spectral resolution have been performed[7,8] as well as multi-colour fluorescence imaging experiments[9]. Further, a fluorescence monitoring system for use with bronchoscopes and cystoscopes has been constructed utilizing contrast enhancement techniques[10]. Below we give an overview of our fluorescence studies of different tissues and discuss potential clincial applications.

Spectroscopic Point Measurements

The set-up used for point measurements in tissue is shown in Fig. 1. For inducing the fluorescence a N_2 laser, emitting 337 nm radiation, was used at a 10 Hz repetition rate. Either a homebuilt system with a pulse length of 10 ns or a Laser Science Model VSL-337 laser, emitting 3 ns pulses was employed. An interference filter with a wavelength of 340 nm was used in the beam to suppress unwanted plasma lines. The light impinging on the target had a pulse energy of about 30 μJ in an illuminated spot of 2-3 mm diameter. A metal ring that was sometimes equipped with a fluorescence-free quartz plate, was used for defining the object plane. LIF passed via a first-surface mirror through an f=15 cm quartz lens and illuminated the entrance slit of a Jobin-Yvon UFS-200 spectrograph with a Tracor Northern TN-1223-4IG intensified diode array detector in the focal plane. The resolution of the system was about 5 nm. The entire U.V.- Visible - near-IR spectral region was captured for each laser pulse in the 25 mm long, 1024 element detector. Signal averaging

could be performed in the TN 1710 main frame and spectra with proper identification were stored on floppy discs. As a fluorescence standard we used a 3 mm thick layer of Rhodamine 6G dye in water (70 µg/litre). All measured fluorescence intensities are expressed in this unit.

In our studies of HPD-bearing tissues we used white inbred female Wistar/Furth rats. A malignant tumour on the right hind leg had been induced by local inoculation of syngeneic tumour cells prepared from a colon adenocarcinoma (DMH-W49)[11]. At the time of animal sacrifice and fluorescence investigation the tumours were about 10 mm in diameter in some measurement series, and about 25 mm in other series. At various times before the investigation the rats had been injected intravenously (v. femoralis) at a level of normally 5 mg/kg body weight with 0.5 mg/ml HPD solution (Photofrin solution, ORD INC. Cheektowaga, N.Y., diluted 10 time in physiological saline).

Spectra were recorded by accumulating data for 80 pulses. The general features are illustrated in Fig. 2. At the top of the figure the fluorescence spectrum for diluted Photofrin solution is shown with peaks at ~610 and ~670 nm. Fig. 2b shows the spectrum from the surface of the tumour in a rat (skin removed), which had been injected 2 days earlier with HPD. The tumour exhibits very clear HPD features. It is noted that the first peak is shifted to 630 nm and that the second peak has become broadened. Normal muscle (on the other, unaffected leg) lacks the HPD signature (Fig. 2c). In Fig. 2d the spectrum of a non-injected animal is shown. Here some non-specific excess red fluorescence is also obtained. We always evaluate the 630 nm signal level over a smooth background and designate measured signals as indicated in the figure. The results of measurements of the A signal level in different organs are presented with standard deviations in Fig. 3 (Ref. 12). The investigation was performed on animals that had been injected with HPD 2 h, 4 h, 8 h, 1 day, 3 days and 4 days earlier. For each organ the value for control rats (no HPD administration) is indicated as a dashed line with error bars. Each data point is based on measurements on 3-6 animals. The results are in general agreement with our previously published, less extensive data[7].

It is observed that the fluorescence levels are reduced to half their original values over a period of about 3 days. A significantly stronger signal is obtained for the HPD-injected rats compared with the control values for the different tumour tissues.

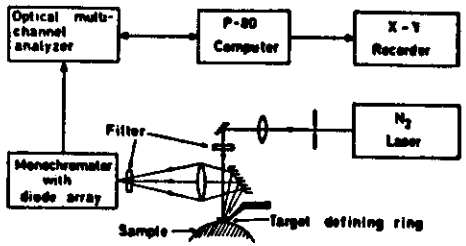

Fig. 1. Experimental arrangement for laser-induced fluorescence measurements in tissue.

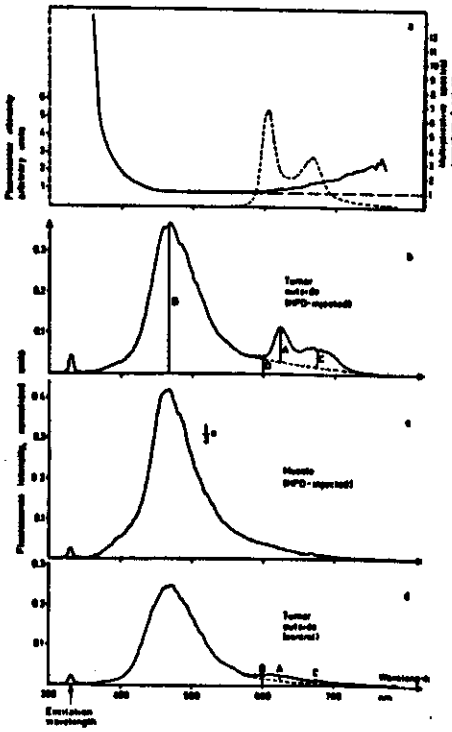

Fig. 2. a) Fluorescehce spectrum of diluted Photofrin solution (broken line). Spectral correction factor (full line). b) Fluorescence spectrum of tumour surface in a rat that had been injected with HPD two days earlier. Signal intensities at characteristic wavelengths are denoted by A, B, C and D. c) Fluorescence spectrum of muscle on unaffected leg for the same rat as in b). Note that the intensity of the curve has been reduced by a factor 2. d) Fluorescence spectrum of a tumour in a rat that had not received an HPD injection. (From Ref. 7.)

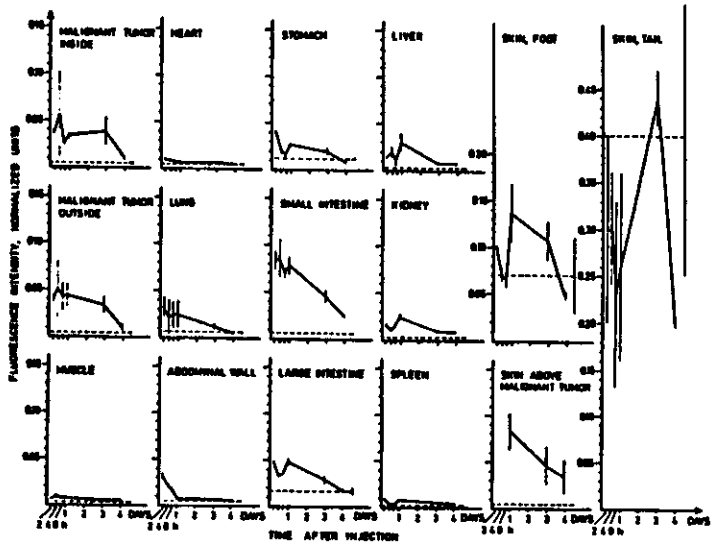

Fig. 3. Fluorescence intensity A in normalized units for different rat tissues. Intensities are shown with standard deviations at different times after the injection of HPD. Note that points corresponding to 2, 4 and 8 hours are plotted on a non-linear time scale. The background level for non-injected rats is indicated by a broken line with error bars. (From Ref. 12.)

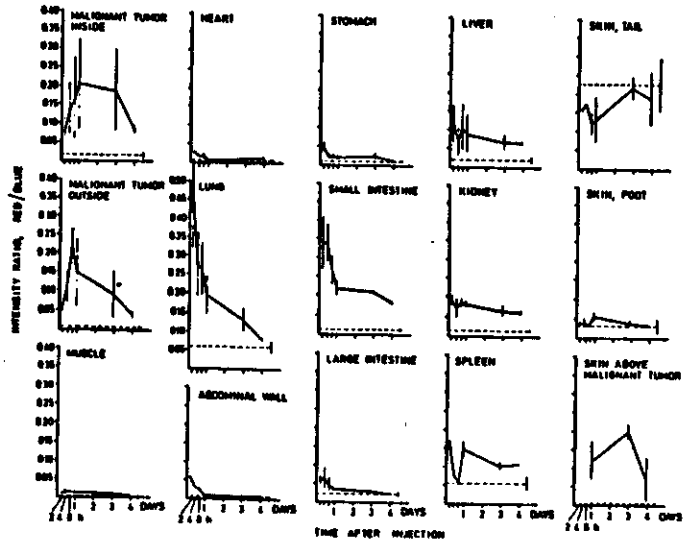

Fig. 4. Ratio of signal intensities A and B (red/blue). The plot has been made in a similar way as in Fig. 3. (From Ref. 12.)

Most important, the tumour tissues have a much higher HPD fluorescence than the unaffected muscle tissue, which is the HPD differentiation effect already observed in Fig. 2. From Fig. 3 it is evident that certain rat organs, in particular the tail skin, contain natural constituents that give rise to a strong non-HPD related A signal. Further, some non-tumour organs such as liver, spleen and the intestines give a high HPD-related signal. However, it is possible to sharpen the discrimination between tumour and normal tissue further by using the shape of the red emission band. The C/A ratio is different for tumour tissue and non-tumour tissue, and with a discrimination level of C/A >0.5, only liver tissue occasionally falls in the same category as tumour tissue.

In the measurements it was noted that the blue fluorescence intensity was considerably weaker in the rat tumour tissue than in normal muscle tissue. This can be observed in Fig. 1 at the blue peak at about 470 nm (peak B). Thus, contrast between the two types of tissue can be enhanced by forming the ratio A/B. In Fig. 4 this ratio, which in the same way as the C/A ratio, has the advantage of being dimensionless and thus independent of intensity calibrations, is plotted for the same rat organs as in Fig. 3 with standard deviations and control-animal ratios[12]. Indeed, very good discrimination between tumour and normal muscle tissue is obtained as seen in the left part of the figure. However, several other organs also have a high A/B ratio. The very opaque organs like the kidneys and the spleen have low A values although they are known to have high HPD concentrations[1]. In the ratio A/B the opacity influence is reduced.

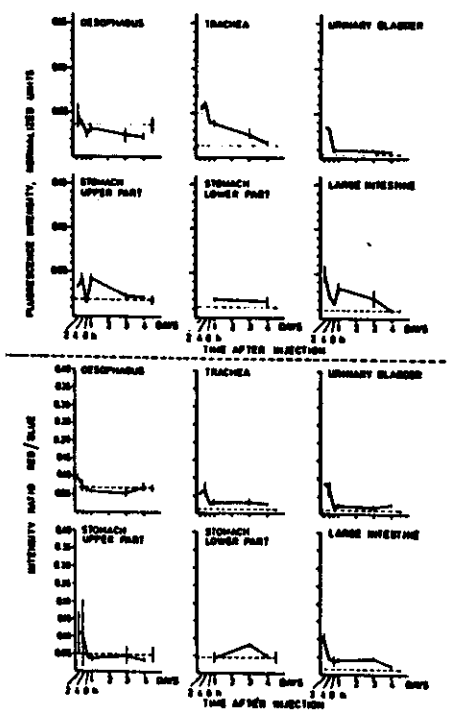

Fig.5. Results for signal levels A and A/B for organs accessible with endoscopic techniques (rat tissue, inner walls). (From Ref. 12.)

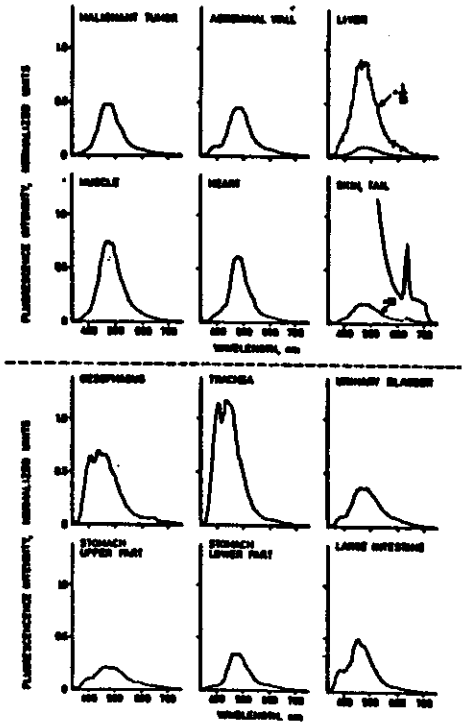

Fig. 6. Spectrally uncorrected natural fluorescence curves for 12 types of rat tissue. (From Ref. 13.)

For discriminating tumour tissue from other tissue it is desirable to form an optimum contrast function. By carefully comparing Figs. 3 and 4 it is observed that increased contrast can be obtained by multiplying the two functions by each other, i.e. to form the function A^2/B. Non-tumour tissue with a high A^2/B value has a lower C/A value than tumour tissue. By setting simultaneous criteria for A^2/B and C/A or for A/B and C/A, tumour tissue can be efficiently distinguished from healthy tissue.

Above we have discussed the HPD signature in different tissues with emphasis on the possibility of automatically selecting tumour tissue. The properties of the inner walls of organs that are accessible by endoscopic techniques, are of special interest. In Fig. 5 the results for such organs are presented both in terms of the A and the A/B values[12]. Contrast enhancement techniques are clearly of great interest for tumours growing on accessible inner walls.

It is necessary to characterize the normal tissue fluorescence as closely as possible, since this fluorescence will be the background against which tumours will be detected. We have made a detailed statistical investigation of this background fluorescence[13]. In Fig. 6 typical fluorescence curves for 12 types of rat tissue are shown on the same intensity scale. The curves are not spectrally corrected.

We have also investigated certain human tissue samples with regard to fluorescence. A large number of biopsy specimens from skin tumours have been studied. The samples were mainly skin naevi and fibromas but basal-cell carcinomas and histiocytomas were also represented. At the present time the number of investigated malignant samples is too low to allow any conclusions to be drawn. In Fig. 7 spectra from 3 different human skin specimens are shown[13]. Human brain tumours are also being investigated. In Fig. 8 spectra of normal and malignant brain tissue are shown[14].

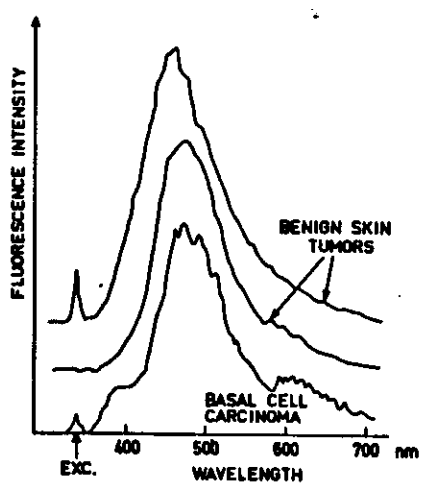

Fig. 7. Fluorescence spectra of human skin tumours (From Ref. 13).

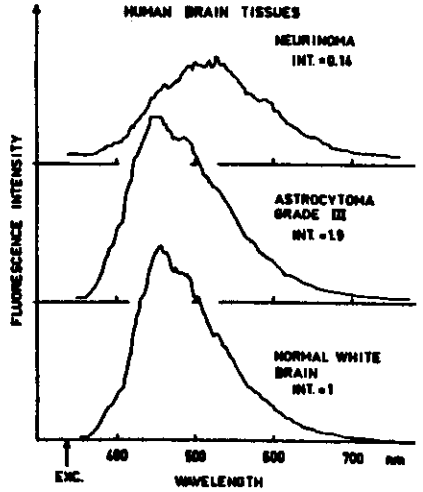

Fig. 8. Fluorescence spectra of human brain tissue (From Ref. 14).

Multi-colour fluorescence imaging

As illustrated above, properly treated data from LIF studies provide valuable information on tumours. The measurements discussed so far were performed by observing the whole fluorescence spectrum at selected points in the various tissues. Clearly, it would be desirable to obtain fluorescence "images" that carry the same type of information but with spatial resolution. The results of the first step along these lines are shown in Fig. 9, in which spectra taken at 8 points (diam. 2 mm) along a straight line starting in healthy muscle and extending into an induced rat tumour are shown recorded with the set-up shown in Fig. 1. Evaluated signal levels are shown in the lower part of the Figure. The reduction in blue fluorescence light in the tumour region is very evident. The importance of isolating

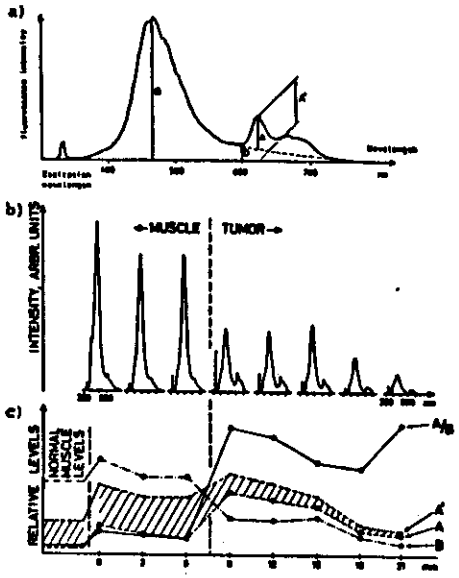

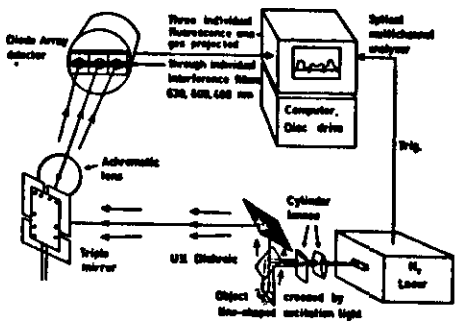

Fig. 10 (above). Experimental arrangement for spatially resolved multi-colour LIF measurements (From Ref. 9).

Fig. 9 (left). a) Typical fluorescence spectrum of tumour in a rat injected with HPD. b) Fluorescence spectra at 8 points along a line extending from muscle into the tumour. c) Evaluated signal levels.

the specific HPD signal, A, from the background (A'-A) is illustrated. A recording of the total intensity A' shows little contrast, while the A curve shows the tumour boundary. As already discussed above, further contrast enhancement is obtained by measuring the dimensionless ratio A/B. Measurements of this kind give good insight into tissue fluorescence characteristics but require tedious recording and data processing. In order to make such measurements easier we have developed a multi-colour fluorescence-imaging technique, in which full contrast enhancement can be retained in spatially resolved representations[9]. In Fig. 10 the set-up is illustrated. Using cylinder lenses, a N_2 laser beam is shaped to a 20 mm long and 1 mm wide line at the position of the object. The object plane is defined by a fluorescence-free quartz plate against which the object is placed from below. A three-mirror arrangement and a common achromatic lens are used for forming three individual images of the streak of LIF that is emitted by the object. By adjusting the mirrors the three images (demagnified by a factor of 4) are put side by side, and the intensified linear-array detector, that was discussed above, is placed at the three-fold image line position. An interference filter arrangement, selecting 5-10 nm wide bands at 630, 600 and 488 nm was placed in front of the array, allowing spatially resolved LIF to be detected in these three bands. Although single-pulse measurements with good signal-to-noise ratio were possible, data were normally accumulated from 50 pulses. Because of the gated action of the image intensifier in the detector arrangement, measurements could be made in full ambient illumination. The measurement technique is illustrated in Fig. 11. Here the image line is placed across a rat tumour of 10 mm diameter with a central necrosis. In this particular case only 0.5 mg/kg HPD was injected 2 days before the investigation. In part (a) of the Figure the response function of the system is shown in the different spectral bands. (The recording was made on paper exhibiting white fluorescence.) The profiles result from the laser beam light distribution, some vignetting in the lens and from the variation in response along the detector. From the curves, multiplicative correction functions are determined, which, when applied, reduce the recorded data to the idealized "flat" response curve. Raw recordings of the tumour fluorescence are shown in (c). Excess red fluorescence is found both in the 630 (A') and 600 nm (D) bands, whereas the blue response (B) is more flat. Below, curves multiplied by the correction functions are shown (d). In order to remove the specific HPD fluorescence, A, from the background, which is also included in the measured A' curve, we subtract the D curve (600 nm), multiplied by a factor k, from the A' curve as illustrated in (e). The value of the factor k is obtained by comparing imaging measurements of this kind with corresponding point-wise spectrally resolved measurements for the same samples. In the lower part of the figure (f) a comparison between imaging and sequential measurements of A and B is shown with quite good agreement. In Fig. 12 some

examples of contrast enhancement by properly subtracting 600 nm curves from 630 nm curves are shown. Although the correct multiplicative factor to be used in the subtraction can be found with the procedure indicated above, an alternative, straightforward procedure for contrast enhancement is adopted here by simply multiplying the D curve by a factor k chosen to fit the A' and D curves in the non-tumour region. The tumour region then shows up in the subtraction because of its excess 630 nm light. In the cases shown in the upper row of Fig. 12, 5 mg/kg HPD had been injected whereas only 0.5 mg/kg was used for the lower-row cases

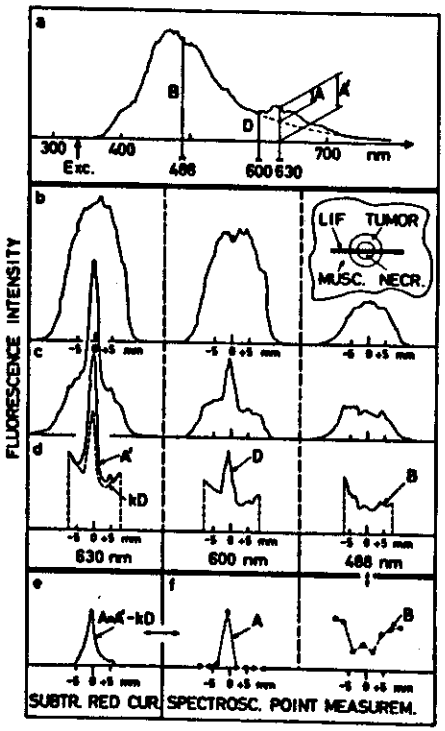

Fig. 11. For explanations, see text! (Ref. 9.)

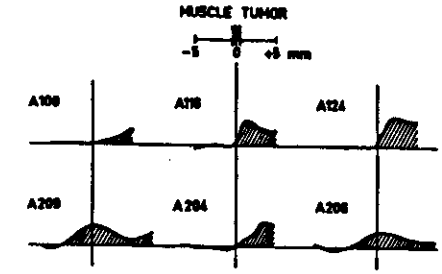

Fig. 12. Examples of contrast enhancement at tumour edges obtained by fitting D and A' curves in the (distant) non-tumour region with subsequent subtraction of the D curve. Rats were injected by 5 mg/kg bodyweight HPD 1-3 days before the investigation for upper row curves, and with only 0.5 mg/kg for the lower row. (From Ref. 9.)

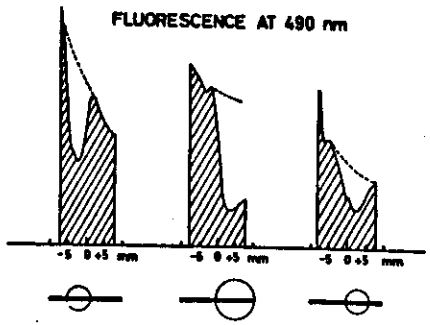

Fig. 13. Imaging recordings of blue fluorescence in connection with cancer tumours on muscle.

The blue fluorescence has not been utilized in any of the cases discussed in Figs. 11 and 12. As we have mentioned above the blue fluorescence decreases in the tumours investigated here compared with the surrounding muscle. This is illustrated in some spectra recorded from tumours on muscle background in Fig. 13. Here the tumour shows up as a prominent "blue hole". Red and blue information is combined in the formation of an A/B ratio. A particularly difficult case is shown in Fig. 14. In this case red as well as blue fluorescence is strongly attenuated for the tumour because of its heavy superficial blood staining. The corrected curves are given in the upper row and the properly subtracted curve yielding the A distribution is shown in panel (b). Only in the A/B ratio does the tumour boundary emerge. Clearly, the imaging techniques discussed here can be extended to two-dimensional monitoring and adaptation to endoscopic equipment.

Endoscopic Fluorescence Equipment

The techniques for contrast enhancement in cancer tumour localisation discussed in this paper can be adapted for practical/clinical endoscopic work. At the Lund Institute of

Technology an instrument of the general working principle described in Ref. 15 has been constructed[10]. A schematic diagram of the system is shown in Fig. 15. A 200 W high-pressure mercury lamp is used for normal endoscope illumination as well as for violet-light excitation Employing a rotating filter and chopper wheel, intermittent functions are in operation. During the white light illumination phase a normal endoscopic function is obtained. When the wheel is further turned an interference filter isolates violet-light excitation and a photomultiplier tube is exposed to the fluorescence through a red filter. The photomultiplier is then again blocked during a new white-light excitation period. In contrast to the original version[15], the present instrument also detects blue-green fluorescence light during the fourth and last part of a measurement cycle. The cycle is run at 17 Hz producing only a slight visual flicker for the endoscopist. A microprocessor is used for evaluating the A'/B ratio and a change in the pitch of an audio-oscillator is obtained when the A'/B ratio changes, e.g. because of the presence of a tumour. First tests with an Olympus bronchoscope are planned.

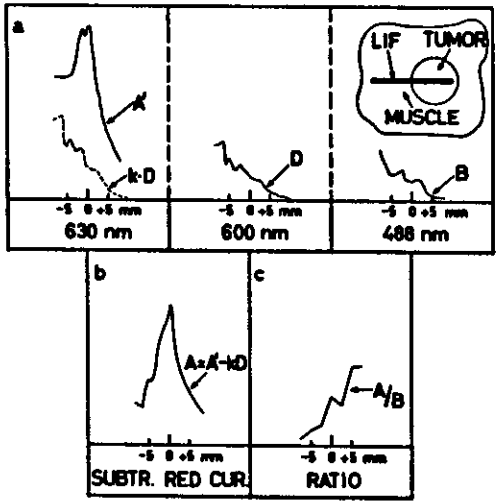

Fig. 14. Recordings of fluorescence along a tissue line extending from muscle to blood-stained tumour. 5 mg/kg bodyweight HPD was injected 1 day before the investigation. a) corrected fluorescence curves. b) "A" curve obtained by subtraction of "red" curves. c) A/B ratio curve. (From Ref. 9)

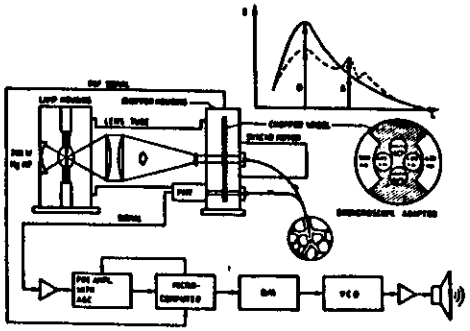

Fig. 15. Fluorescence endoscope constructed at the Lund Institute of Technology. (From Ref. 10).

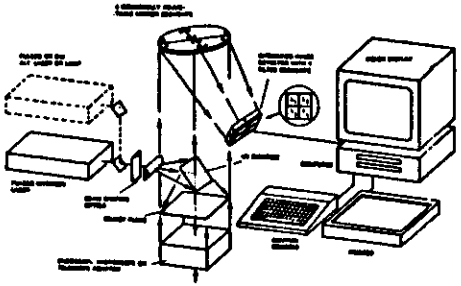

Fig. 16. Proposed computer-enhanced multi-colour fluorescence-imaging system. (Ref. 17).

In many medical applications imaging systems are desirable. An endoscopic system for fluorescence imaging has been developed by Profio et al[16]. A computer-enhanced multi-colour fluorescence-imaging system recently proposed[17] is illustrated in Fig. 16. This instrument operates on the principles given in Fig. 10, but it generates 2-D contrast-enhanced images. Using a segmented spherical mirror, 4 filtered images are simultaneously recorded with a diode matrix or Vidicon detector. Using dimensionless optimum contrast functions such a system can produce enhanced picture information on faint features, while still being immune to fluctuations and non-uniformities in the illumination as well as to topographical effects in the target material. With an endoscopic adaptor such a system equipped with a powerful computer system should provide near real-time information on faint fluorescence anomalies associated with the presence of cancer tumours.

Acknowledgments

The support of the Lund University HPD working group is gratefully acknowledged. Financial support was provided by the Swedish Cancer Foundation (RmC)

References

1. T.J. Dougherty, CRC Critical Reviews in Oncology/Hematology, S. Davis, Ed. CRC Press (Florida 1984).
2. J.H. Kinsey, D.A. Cortese and D.R. Sanderson, Mayo Clin. Proc. 53, 594 (1978).
3. E.G. King, G. Man, J. le Riche, R. Amy, A.E. Profio and D.R. Doiron, Cancer 49, 777 (1982).
4. D. Jocham, G. Staehler, Ch. Chaussy, C. Hammer and U. Löks, Urologie A 20, 340 (1981).
5. A. Tsuchiya, M. Obara, M. Niwa, T. Ohi, H. Kato and Y. Hayata, J. Urol. 130, 79 (1983).
6. K. Svanberg and S. Svanberg, Lund Reports on Atomic Physics LRAP-23 (1983).
7. J. Ankerst, S. Montán, K. Svanberg and S. Svanberg, Appl. Spectr. November 1984
8. J. Ankerst, S. Montán, K. Svanberg and S. Svanberg, Proc. CLEO '84, J. Opt. Soc. Am. B 1, 558 (1984).
9. S. Montán, K. Svanberg and S. Svanberg, to be published.
10. S. Andersson and T. Persson, Diploma paper, Lund Institute of Technology, Lund Reports on Atomic Physics LRAP-39, (1984), in press.
11. G. Hedlund and H.O. Sjögren, Int. J. Cancer 26, 71 (1980).
12. J. Ankerst, L. Kjellén, S. Montán, E. Sjöholm, K. Svanberg and S. Svanberg, to be published.
13. S. Montán, K. Svanberg and S. Svanberg, to be published.
14. S. Montán and L.G. Strömblad, (unpublished).
15. J.H. Kinsey and D.A. Cortese, Rev. Sci. Instr. 51, 1403 (1980).
16. D.R. Doiron, E. Profio, R.G. Vincent and T.J. Dougherty, Chest 76, 27 (1979); E. Profio et al. in A. Andreoni and R. Cubeddu, Eds., Porphyrins in Tumour Phototherapy, Plenum Press (New York 1984).
17. S. Montán and S. Svanberg, (unpublished).

TISSUE DIAGNOSTICS USING LASER-INDUCED FLUORESCENCE TECHNIQUES

P.S. Andersson, J. Ankerst*, E. Kjellén*, S. Montán,
K. Svanberg* and S. Svanberg

Department of Physics, Lund Institute of Technology,
P.O. Box 118, S-221 00 Lund, Sweden

*Lund University Hospital, S-221 85 Lund, Sweden

Invited paper
at the
Second International Laser Science Conference
Seattle, October 20-24, 1986

TISSUE DIAGNOSTICS USING LASER-INDUCED FLUORESCENCE TECHNIQUES

P.S. Andersson, J. Ankerst*, E. Kjellén*, S. Montán,
K. Svanberg* and S. Svanberg
Department of Physics, Lund Institute of Technology,
P.O. Box 118, S-221 00 Lund, Sweden

*Lund University Hospital, S-221 85 Lund, Sweden

ABSTRACT

The fluorescence emission from tissue that is irradiated with UV-light can be utilized for diagnostic purposes. The discrimination between tumors and normal tissue is of particular interest. We discuss natural tissue fluorescence as well as fluorescence due to injected hematoporphyrin agents. Results from studies on rats and mice are reported, as well as data from human biopsy samples. The development of clinical instrumentation for point measurements and imaging is discussed.

INTRODUCTION

Fluorescence monitoring of tissue is emerging as a promising technique for non-intrusive real-time diagnostics, e.g. for tumor localization. For some time the specific red fluorescence from previously injected tumor-seeking hematoporphyrin derivative (HPD) molecules has been used for such purposes. Recent progress in the field of tumor localization using HPD is described in the Proceedings of the First International Conference on the Applications of Photosensitization for Diagnosis and Treatment[1]. However, even without any agent injection tissue exhibits certain features in the fluorescence spectrum that can be used for tissue characterization. Several studies of this auto-fluorescence have been performed by our group[2-4] and others[5-6]. It seems that a combined use of auto-fluorescence and HPD features is particularly useful for tumor detection. We have shown that an enhanced contrast between tumor and surrounding muscle can be obtained for an experimental rat tumor system by dividing the background-free HPD fluorescence intensity by the blue tissue auto-fluorescence[7-9]. The tumor was found to be characterized by an increase in the HPD signal at the same time as the blue fluorescence decreased. Monitoring a ratio or any other dimensionless quantity also has important advantages, in particular in endoscopic (fiber-optic) applications:

1. Immunity to distance variations
2. Immunity to surface topography
3. Immunity to variations in excitation or detection efficiency
4. Immunity to wavelength-independent attenuation

Fluorescence measurements can be performed with a point monitoring device or with an imaging instrument. Recently part of the available instrumentation has been revieved[10]. Point monitors can either be of filter type[11-13] or can employ optical multichannel

analyzer techniques for full spectrum recovery[14]. The simplest type of fluorescence imaging is visual inspection of the UV-illuminated region. Electronic images can be obtained using intensified vidicon or diode matrix detectors[15], that detect the red fluorescence light in a selected passband. In one construction background can be intermittently subtracted by switching to a blue-transmitting filter[16]. Simultaneous monitoring in several selected bands and subsequent forming of an optimized dimensionless contrast function is possible using the computer-enhanced multi-color fluorescence imaging concept[9,3,17].

Fluorescence monitoring of tissue has mostly been focussed on cancer tumor detection. An emerging application is vessel characterization in connection with laser-based angioplasty[4]. In the present paper we will mostly discuss the former application but we will also present some results from our first studies related to the second field. Recent laboratory results from rats and mice are presented as well as some human biopsy specimen observations.

FLUORESCENCE MONITORING

Throughout this paper laser-induced fluorescence data are presented that have been obtained with an experimental set-up of the type shown in Fig. 1. In most of our studies an N_2 laser emitting light at 337 nm has been employed, but a XeCl (308 nm) excimer laser

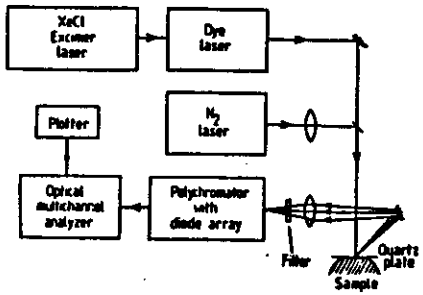

Fig. 1. Experimental set-up used in the studies of tissue fluorescence.

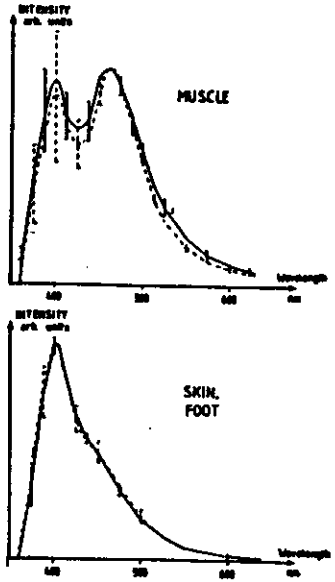

Fig. 2. Auto-fluorescence spectra of muscle fascia and skin of mouse. The full lines correspond to live animals and the dashed ones to dead animals, about 4 hours after sacrifice. Error bars indicate one standard deviation. (Ref. 4).

and an excimer-pumped dye laser have also been utilized. The radiation is directed onto the sample by means of mirrors. Fluorescent light is collected and directed to an optical multichannel analyzer system, that captures the entire fluorescence light distribution for every laser pulse. Spectra can be stored on floppy disks and be printed out on paper. Fluorescence intensities are measured in terms of a standard.

Extensive data on the fluorescence of different tissues of rat at various times after the injection of HPD have been presented in our previous papers[7,8]. In order to ascertain the validity of the approach used we have compared the fluorescence properties of live tissue and the tissue of animals that were sacrificed a few hours earlier[4]. Clearly, it is much easier to perform systematic fluorescence studies on sacrificed animals. In Fig. 2 comparative data for nude mice, first anesthetized with chloral hydrate and then sacrificed are shown. As can be seen the spectral features remain basically the same after sacrifice.

HPD molecules have their strongest absorption in the Soret band around 405 nm. For this reason violet excitation has normally been used to induce fluorescence. However, the contrast attainable between tumor and surrounding normal tissue for a certain injected dose of HPD is even more important than a strong fluorescence intensity. To enhance the contrast we also use the blue tissue auto-fluorescence, which also depends strongly on the excitation wavelength. We have performed extensive studies on induced tumors in Wistar/Furth rats using excitation wavelengths ranging from 308 to 405 nm[18]. In order to assess the contrast, scans extending from normal tissue into the tumor were performed. As an example such a scan for 337 nm excitation is shown in Fig. 3. In the inserted spectrum the relevant signal levels are denoted. In this scan it can be seen that by monitoring the characteristic HPD fluorescence intensity at 630 nm (A') low contrast is achieved. By subtracting the background and plotting the A level the situation is much improved. Rather than displaying a general fall-off in the blue fluorescence intensity (B) for the tumor the intensity falls off in particular at the tumor edges. In an A/B representation a high contrast is achieved and the tumor edges are strongly enhanced. The manual scan indicates what would be achievable with an imaging system. The full material is now being evaluated. In these studies we noted that a strong exposure to laser light can lead to sample bleaching thus changing the fluorescence characteristics. We have noted that an additional peak, at about 650 nm, can be induced in this way. Such a peak has previously been observed and utilized in human tumor detection[19].

An important aspect of tissue fluorescence characteristics is possible guidance in assessing radicality in surgical tumor resection. Here the real-time capability of the fluorescence technique is of particular interest. We have studied a rat brain tumor system and find very encouraging results[20]. In Fig. 4 the results from a scan across the tumor are shown. 337 nm excitation is used in the measurement on rats that were injected with Photofrin II three days earlier. We again note, that background-free HPD monitoring strongly enhances the contrast, which is still further enhanced by normalizing to the

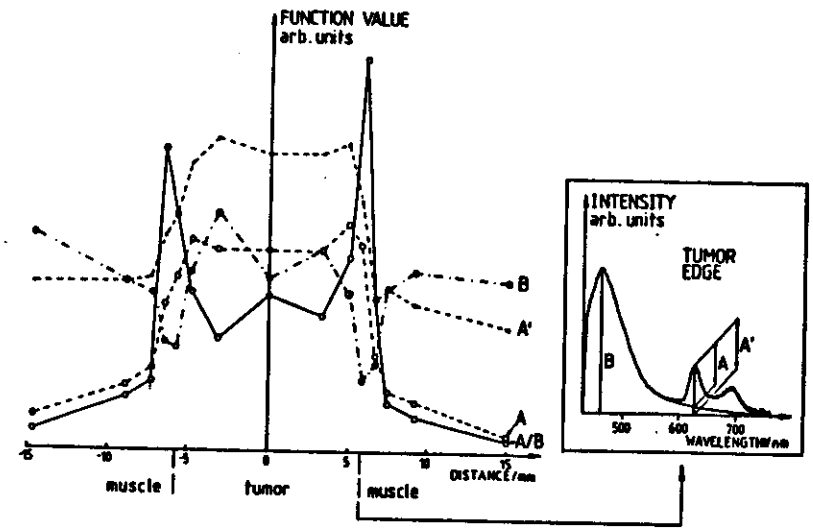

Fig. 3. Fluorescence results from a scan across a rat tumor in muscle.

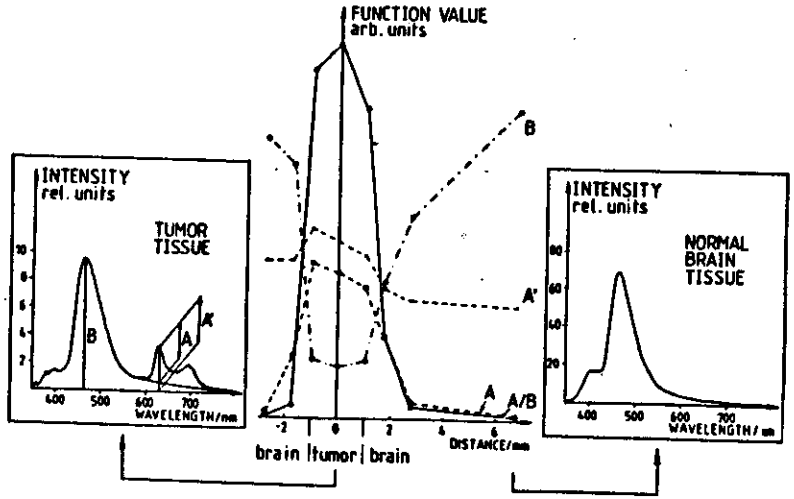

Fig. 4. Results from a scan across a tumor in rat brain. (Ref. 20).

blue fluorescence, which is strongly reduced for the tumor tissue. In the A/B representation a contrast of about 80 is achieved. The data in the figure were obtained using the low dose of 1 mg/kg bodyweight of the drug.

Recently the photodynamically more potent drug Photofrin II was introduced. This agent is enriched in DHE (dihematoporphyrin ether), which has been shown to be the most active porphyrin component in the previously used deriviative prepared by a modified Lipson procedure (Photofrin). It is well known that porphyrin dimers fluoresce much more weakly than monomers. Studies on saline solutions of Photofrin and Photofrin II solutions show[21], that the fluorescence is basically due to the monomeric "impurity" hematoporphyrin HP, and that the more pure substance Photofrin II exhibits a 3 times lower characteristic red fluorescence. However, in tissue strong transformational processes occur between the porphyrins. In order to evaluate the relative merits of the two agents with regard to tumor localization using fluorescence we have performed a comparative study on Wistar/Furth rats with inoculated tumors[22]. Groups of rats were injected with the same dose of the two agents in a blind test. In tissue Photofrin II gives rise to stronger specific fluorescence than Photofrin for the same injected drug concentration. However, since the more pure substance is injected at a reduced concentration (for cost and skin photosensitization reasons) it is not clear that the pure drug has an advantage over the previous one for the detection of tumors. We also observe a tendency towards reduced contrast for DHE since the non-tumor tissues seem to yield a relatively higher specific red fluorescence than for HPD. Clearly, these indications have to be further studied for definite assessment.

In Fig. 5 some results from our first experiments on fluorescence characterization of vessel status are given[23]. Different samples from a newly deceased 65 year-old person were studied using 337 nm excitation. Clear spectral differences between normal artery wall and wall modified by atherosclerotic plaque were found including the differences in the 550-600 nm region previously reported by Kittrell et al.[4]. Radiation at 337 nm has a much lower penetration depth than at 480 nm, the wavelength used in Ref. 6., and this has to be considered when interpreting the data. We plan to perform more extensive studies of this kind at different excitation wavelengths.

DISCUSSION

Fluorescence diagnostics of tissue has an interesting potential as a clinical aid both for localizing small occult cancer tumors and for ensuring radicality in surgical tumor resection. The full utilization of the available spectral information is important, particularly in the battle to keep the concentration of agents also causing ambient light hypersensitization at the lowest possible level. Tissue auto-fluorescence also provides interesting possibilities outside the tumor localization area. The development of powerful equipment, in particular with imaging capability, using extended spectral pattern recognition approaches seems to be a particular challenge.

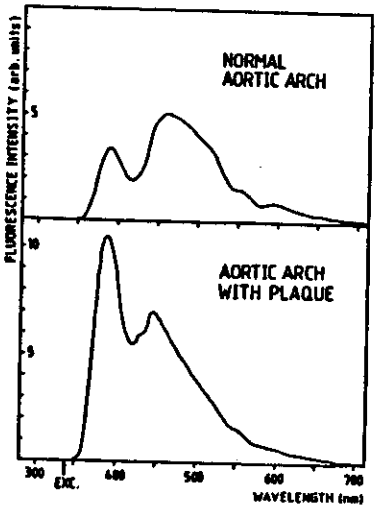

Fig. 5. Comparison between the fluorescence spectra from normal and damaged human aortic arch tissue. For 337 nm excitation, plaque was found to be characterized by a sharp peak at 450 nm and a reduced structure in the 550-600 nm region. (Ref. 23).

ACKNOWLEDGMENTS

The authors gratefully acknowledge valuable discussions with and encouragement from the other members of the Lund HPD Group. This work was supported by the Swedish Cancer Foundation (RmC) and the Swedish Board for Technical Developments (STUF).

REFERENCES

1. Y. Hayata (ed).. Proceedings of the First International Conference on the Applications of Photosensitization for Diagnosis and Treatment, Tokyo, April 30 - May 2, 1986, to appear.
2. S. Montán, Diploma Paper, Lund Reports on Atomic Physics LRAP-17, 1983.
3. J. Ankerst, S. Montán, E. Sjöblom, K. Svanberg and S. Svanberg, L.I.A. ICALEO 84, 43, 52 (1984).
4. P.S. Andersson, E. Kjellén, S. Montán, K. Svanberg and S.Svanberg, to appear.
5. Yanming Ye, Yuanlong Yang, Yufen Li and Fuming Li, CLEO'85 Technical Digest, p. 84.
6. C. Kittrell, R.L. Willett, C. de los Santos-Pacheo, N.B. Ratliff, J.R. Kramer, E.G. Malk, and M.S. Feld, Appl. Opt. 24, 2280 (1985).
7. J. Ankerst, S. Montán, K. Svanberg and S. Svanberg, Appl. Spectr. 38, 890 (1984).
8. K. Svanberg, E. Kjellén, J. Ankerst, S. Montán, E. Sjöblom, and S. Svanberg, Cancer Res. 46, 3803 (1986).
9. S. Montán, K. Svanberg, and S. Svanberg, Opt. Lett. 10, 56 (1985).
10. H. Kato and D. Cortese, Clinics in Chest Medicine 6,237 (1985).
11. J.H. Kinsey and D.A. Cortese, Revs. Sci. Instr. 51, 1403 (1980).
12. P.S. Andersson, S.E. Karlsson, S. Montán, T. Persson, S. Svanberg and S. Tapper, to appear.
13. A.E. Profio, D.R. Doiron and J. Sarnaik, Med. Phys. 11, 516 (1984).
14. K. Aizawa et al. in Porphyrin Localization and Treatment of Tumours, (Alan R. Liss 1984) p. 227.
15. A.E. Profio, D.R. Doiron, O.J. Balchum and G.C. Huth, Med. Phys. 10, 35 (1983).
16. A.E. Profio, M.J. Carvlin, J. Sarnaik and L.R. Wudl, in Porphyrin in Tumor Phototherapy, Eds. A. Andreoni and R. Cubeddu (Plenum 1984) p. 321.
17. S. Montán and S. Svanberg, Patent pending.
18. P.S. Andersson, J. Ankerst, S. Montán, K. Svanberg and S. Svanberg, to appear.
19. M. Yamashita, M. Nomura, S. Kobayashi, T. Sato and K. Aizawa, IEEE J. Quant. Electr. QE-20, 1363 (1984).
20. P.S. Andersson, E. Kjellén, L.G. Salford, K. Svanberg and S. Svanberg, to appear.
21. R. Pottier, J.P. Laplante, Y.-F. Chow, and J. Kennedy, Can. J. Chem. 63, 1463 (1985).
22. P.S. Andersson, J. Ankerst, S. Montán, K. Svanberg and S. Svanberg, to appear.
23. P.S. Andersson, A. Gustafson, U. Stenram, K. Svanberg and S. Svanberg, unpublished results.